NASA TN D-993

TECHNICAL NOTE

D-993

STATIC LONGITUDINAL STABILITY OF A ROCKET VEHICLE HAVING A REAR-FACING STEP AHEAD OF THE STABILIZING FINS

By Robert J. Keynton

Langley Research Center
Langley Air Force Base, Va.

NATIONAL AERONAUTICS AND SPACE ADMINISTRATION
WASHINGTON
November 1961

A

NATIONAL AERONAUTICS AND SPACE ADMINISTRATION

TECHNICAL NOTE D-993

STATIC LONGITUDINAL STABILITY OF A ROCKET VEHICLE HAVING A REAR-FACING STEP AHEAD OF THE STABILIZING FINS

By Robert J. Keynton

SUMMARY

Tests were conducted at Mach numbers of 3.96 and 4.65 in the Langley Unitary Plan wind tunnel to determine the static longitudinal stability characteristics of a fin-stabilized rocket-vehicle configuration which had a rearward facing step located upstream of the fins. Two fin sizes and planforms, a delta and a clipped delta, were tested. The angle of attack was varied from 6° to -6° and the Reynolds number based on model length was about 10×10^{6}.

The configuration with the larger fins (clipped delta) had a center of pressure slightly rearward of and an initial normal-force-curve slope slightly higher than that of the configuration with the smaller fins (delta) as would be expected.

Calculations of the stability parameters gave a slightly lower initial slope of the normal-force curve than measured data, probably because of boundary-layer separation ahead of the step. The calculated center of pressure agreed well with the measured data. Measured and calculated increments in the initial slope of the normal-force curve and in the center of pressure, due to changing fins, were in excellent agreement indicating that separated flow downstream of the step did not influence flow over the fins. This result was consistent with data from schlieren photographs.

INTRODUCTION

Wind-tunnel tests were conducted in the Langley Unitary Plan wind tunnel on a 0.10-scale model of the second and third stages of a proposed three-stage rocket vehicle. This configuration had a large conical frustum located midway along the body which produced a rearward facing step. It was believed that the flow downstream of the step might separate and have an adverse effect on the flow over the

rear stabilizing fins. The tests therefore were conducted to determine the effect of this step on the static longitudinal stability characteristics of the vehicle.

The model was tested with two sets of wedge fins having different areas, planforms, and wedge angles. The larger fin was a clipped delta with a leading-edge sweep angle of 60° and a total wedge angle of 5.4°. The delta fin, which had an area approximately 28 percent less than that of the clipped delta, had a leading-edge sweep angle of 70° and a total wedge angle of 2.9°. Mach numbers for the tests were 3.96 and 4.65 at Reynolds numbers of 9.55×10^6 and 12.83×10^6, respectively, based on model length. Angle-of-attack variations were from 6° to -6°. Schlieren photographs were taken to determine the extent of flow separation.

Calculations of the static longitudinal stability characteristics were made and are compared with the test results.

COEFFICIENTS AND SYMBOLS

The force and moment coefficients of the model are referred to a body system of axes. Positive directions of force and moment coefficients and angles are shown in figure 1. The moment coefficients are presented about a moment center located 9.12 inches (2.94 body diameters) forward of the model base.

Symbols used in this paper are defined as follows:

A model reference area (maximum cylindrical cross-sectional area or base area), 0.0525 sq ft

C_A axial-force coefficient, $\frac{\text{Axial force}}{qA}$

$C_{A,b}$ base axial-force coefficient, $\frac{\text{Base axial force}}{qA}$

C_m pitching-moment coefficient, $\frac{\text{Pitching moment}}{qAd}$

$C_{m,o}$ pitching-moment coefficient at $\alpha = 0^\circ$

C_{m_α} pitching-moment-curve slope, $\frac{\partial C_m}{\partial \alpha}$

C_N	normal-force coefficient, $\frac{\text{Normal force}}{qA}$
C_{N_α}	normal-force-curve slope, $\frac{\partial C_N}{\partial \alpha}$
d	reference length (maximum cylindrical diameter, 3.1 inches)
M	Mach number
q	dynamic pressure, lb/sq ft
x_{cp}/d	nondimensional center-of-pressure location measured from model base
x_{mc}	distance from model base to moment center, 9.12 in.
α	angle of attack, deg

TUNNEL AND APPARATUS

The tests were conducted in the high Mach number test section of the Langley Unitary Plan wind tunnel. The test section is 4 feet square and approximately 7 feet long. The nozzle leading to the test section is an asymmetric sliding-block type. The Mach number may be varied from 2.3 to 4.7 without tunnel shutdown. A complete description of the Unitary Plan wind tunnel may be found in reference 1.

Forces and moments were measured by means of a six-component electrical strain-gage balance, which was internally mounted. The balance was attached by means of a sting to the tunnel central support system. Angle-of-attack tests were made by means of a remotely operated, adjustable angle coupling included in the tunnel central support system. Schlieren photographs were also obtained.

MODEL AND TESTS

Dimensional details of the model are given in figure 2(a). The model was tested with two sets of fins having different planforms, areas, and total wedge angles as shown in figure 2(b). A photograph of the model is shown in figure 3. The configuration having the clipped delta fin was tested at M = 4.65 and 3.96; the delta-fin configuration was

tested only at $M = 4.65$. A transition strip of No. 60 carborundum grains was glued to the model three-fourths of an inch from the nose as shown in figure 3 to insure turbulent boundary layer over the body.

The model was tested through an angle-of-attack range of 6° to -6° at an angle of sideslip of 0°. The stagnation temperature was 175° F and the dewpoint was held at -30° F to prevent condensation. The tunnel test conditions which varied are listed in the following table:

Mach number	Stagnation pressure, lb/sq in. abs	Dynamic pressure, lb/sq ft	Reynolds number based on model length
3.96	59	683	9.55×10^6
4.65	109	649	12.83×10^6

CORRECTIONS AND ACCURACY

All angle-of-attack results presented herein have been corrected for flow misalinement and sting-balance deflections due to aerodynamic load. The flow-angle corrections applied to the data were determined at a station approximately midway along the model length. The upflow present in the test section produces a variation in angle of attack along the body length such that models of this length may show some value of $C_{m,o}$, the pitching-moment coefficient at an angle of attack of 0°, even when the normal force is adjusted to be zero at $\alpha = 0^\circ$.

Even though the level of pitching-moment coefficient would be different if this $C_{m,o}$ were removed, the slopes would not change and therefore the point-to-point increments and slope results discussed herein may be considered accurate. The estimated accuracies of the force and moment coefficients and angle of attack based on balance calibration and repeatability of data are as follows:

ΔC_N	± 0.015
ΔC_m	± 0.010
α, deg	± 0.1

The maximum deviation of local Mach number in the portion of the tunnel occupied by the model is ± 0.045.

The axial-force coefficients have been adjusted to a condition of free-stream static pressure at the base of the model. Typical base axial-force coefficients are presented in figure 4.

RESULTS AND DISCUSSION

Schlieren-Photograph Data

Schlieren photographs were taken of the configuration with the clipped delta fins and are presented in figure 5. Photographs of the model with the delta fins were not obtained.

Two regions of separated boundary layer may be noted in figure 5 at $\alpha = 0^\circ$, one at the juncture of the 13° and 31° frustums and the other at the base of the 31° frustum. The first separated region reattaches at a point about three-quarters of the length of the 31° frustum. The second separated region reattaches about one-quarter of one body diameter downstream of the 31° frustum.

Figure 5 shows that the flow just ahead of the stabilizing fins is attached to the body and that a strong shock wave is present on the leading edge of the fins. Therefore, based on the data from the schlieren photographs, it would be expected that the fins were not affected by the second separated flow region.

Force and Moment Data

Force and moment coefficients for the delta and clipped delta fins are presented in figures 6 to 8. Data were obtained at Mach numbers of 3.96 and 4.65 for the clipped delta fin and at a Mach number of 4.65 only for the delta fin.

The possibility of hysteresis was anticipated (because of separation behind the 31° frustum); therefore, the angle of attack was varied from 0° to -6°, from -6° to 6°, and from 6° to 0° in 1° increments. No hysteresis is evident in figures 6 to 8.

As expected, the effect of increased fin area and wedge angle of the clipped delta fin was an increase in the initial slope of the normal-force curve and a rearward movement of the center of pressure. The increase in the slope was approximately 12.7 percent and the rearward shift in the center of pressure was about 0.20 body diameter. The center of pressure for both configurations tended to move forward as the angle of attack increased. The shift was about 0.20 body diameter from the value at $\alpha = 0^\circ$ over the angle-of-attack range tested. (See fig. 9.)

The solid curves of figure 9 represent the center of pressure as obtained from the following equation:

$$\left(\frac{x_{cp}}{d}\right)_{\alpha=n} = \frac{x_{mc}}{d} + \left(\frac{C_m}{C_N}\right)_{\alpha=n} \tag{1}$$

whereas the dashed curve was obtained from

$$\left(\frac{x_{cp}}{d}\right)_{\alpha=n} = \frac{x_{mc}}{d} + \left(\frac{C_{m_\alpha}}{C_{N_\alpha}}\right)_{\alpha=n} \tag{2}$$

The point at $\alpha = 0^\circ$ was obtained from equation (2) by using values of C_{m_α} and C_{N_α} at $\alpha = 0^\circ$.

The asymmetric appearance of the center-of-pressure curve of the clipped delta fins at $M = 3.96$ is due to upflow present in the test section as is discussed in the section entitled "Corrections and Accuracy." Computation of the center of pressure as a function of angle of attack by the method of slopes (eq. (2)) removes this asymmetry.

The degree to which the separated flow behind the 31° frustum affected the stabilizing fins cannot be determined directly from the measured force and moment data. However, by comparison with calculated data, as shown in the next section, it is possible to deduce a qualitative effect of the separated flow on fin effectiveness.

Calculated Data

By using the method of summation of forces and moments of the various geometric shapes which make up the model configuration, C_{N_α} and x_{cp}/d for the model were calculated as a function of Mach number. The data used in calculating C_{N_α} and x_{cp}/d are both experimental and theoretical and may be found in references 2 to 9.

The following table is a categorization of the geometric shapes with the appropriate references:

Geometric shape	Reference number	
	Initial normal-force-curve slope	Center of pressure
Cone	2; 3	3; 5
Frustum	2; 5; 6	5; 6
Cylinder	4; 7	4; 7
Fin	8; 9	8; 5

An assumption necessary for the use of the method of summation and the data of references 2 to 9 is that there is no boundary-layer separation over any portion of the body. The effect of separated flow may be accounted for in an approximate manner by adjusting the actual geometry of the vehicle to conform to the geometry of the separation lines (which is, to a first order, the geometry "seen" by the flow). Such a procedure, however, would require a prior knowledge of the separated-flow pattern, achieved by schlieren photographs or arbitrary adjustments based on previous experience. Therefore, the calculated data herein are based on the actual geometry of the configuration.

Only fair agreement between the calculated and measured values of C_{N_α} at $\alpha = 0^\circ$ for the total configuration was obtained for both the clipped delta and delta fins. (See figs. 10(a) and 10(b).) As was noted previously, the schlieren photographs indicated two regions of boundary-layer separation. Reference 10 shows that, for bodies which incorporate conical frustums, boundary-layer separation and subsequent reattachment on the frustum tend to increase C_{N_α}. Since the measured values of C_{n_α} are higher than the calculated values, by about 30 percent at $M = 4.65$, it may be concluded that the boundary-layer separation at the juncture of the two conical frustums is probably the major cause for disagreement between the measured and calculated values of C_{N_α} for the total configuration.

Very good agreement was achieved between the measured and calculated values of x_{cp}/d. (See figs. 10(a) and 10(b).) This agreement was probably somewhat fortuitous since the effect of the boundary-layer separation is not noticeable when considered from the standpoint of the center of pressure because of the proximity of the moment center and the frustums.

The calculated incremental changes in initial C_{N_α} and in x_{cp}/d due to interchanging the clipped delta with the delta fins are in excellent agreement with the experimental incremental changes, as can be deduced from the data in figure 10. These values of ΔC_{N_α} and $\Delta(x_{cp}/d)$ are about 0.016 and 0.2, respectively. Based on the schlieren-photograph data and the agreement between the experimental and calculated values of ΔC_{N_α} and $\Delta(x_{cp}/d)$ for the clipped delta and delta fins, it may be concluded that the separated flow behind the conical step had no effect on the fins.

CONCLUDING REMARKS

A 0.10-scale model of the second and third stages of a proposed rocket vehicle was tested at Mach numbers of 3.96 and 4.65. Two sets of stabilizing fins, a delta and a clipped delta, were tested. The clipped delta fins, which had the greater area and wedge angle, gave the higher initial slope of the normal-force curve and more rearward center of pressure as would be expected. A large conical step, located upstream of the fins, separated the flow just downstream of the step. However, schlieren-photograph data indicated that the region of separated flow was not extensive enough to influence the flow over the fins. Measured results were compared with calculated stability data and the two sets of results were in reasonable agreement. The differences between the calculated and measured data appear to be attributable to the forces induced in the separated region located at the juncture of the two conical frustums (or ahead of the rearward facing step).

Langley Research Center,
National Aeronautics and Space Administration,
Langley Air Force Base, Va., September 27, 1961.

REFERENCES

1. Anon.: Manual for Users of the Unitary Plan Wind Tunnel Facilities of the National Advisory Committee for Aeronautics. NACA, 1956.

2. Staff of the Computing Section, Center of Analysis (Under Direction of Zdeněk Kopal): Tables of Supersonic Flow Around Yawing Cones. Tech. Rep. No. 3 (NOrd Contract No. 9169), M.I.T., 1947.

3. Geudtner, W. J., Jr.: Sharp and Blunted Cone Force Coefficients and Centers of Pressure From Wind Tunnel Tests at Mach Numbers From 0.50 to 4.06. Rep. No. ZA-7-017, Convair, June 16, 1955.

4. Syvertson, Clarence A., and Dennis, David H.: A Second-Order Shock-Expansion Method Applicable to Bodies of Revolution Near Zero Lift. NACA Rep. 1328, 1957. (Supersedes NACA TN 3527.)

5. Truitt, Robert Wesley: Hypersonic Aerodynamics. The Ronald Press Co., c.1959, pp. 86-87.

6. Carraway, Ausley B., Turner, Kenneth L., and Crowder, Janette M.: Effects of Afterbody Shape on the Aerodynamic Characteristics of a Fineness-Ratio-10 Cone-Cylinder Configuration at Mach Numbers From 1.57 to 4.65 Including Design Parameter Curves for Circular Afterbody Flares. NASA TM X-348, 1960.

7. Craft, Joseph C.: Comparison of Second-Order Shock-Expansion Theory With Experimental Data for Cone-Cylinder-Frustum Bodies of Revolution at Supersonic Mach Numbers. ARGMA TN 1G6N, U.S. Army Ord. Missile Command (Redstone Arsenal, Ala.), Dec. 31, 1959.

8. Pitts, William C., Nielsen, Jack N., and Kaattari, George E.: Lift and Center of Pressure of Wing-Body-Tail Combinations at Subsonic, Transonic, and Supersonic Speeds. NACA Rep. 1307, 1957.

9. McLellan, Charles H.: A Method for Increasing the Effectiveness of Stabilizing Surfaces at High Supersonic Mach Numbers. NACA RM L54F21, 1954.

10. Dennis, David H.: The Effects of Boundary-Layer Separation Over Bodies of Revolution With Conical Tail Flares. NACA RM A57I30, 1957.

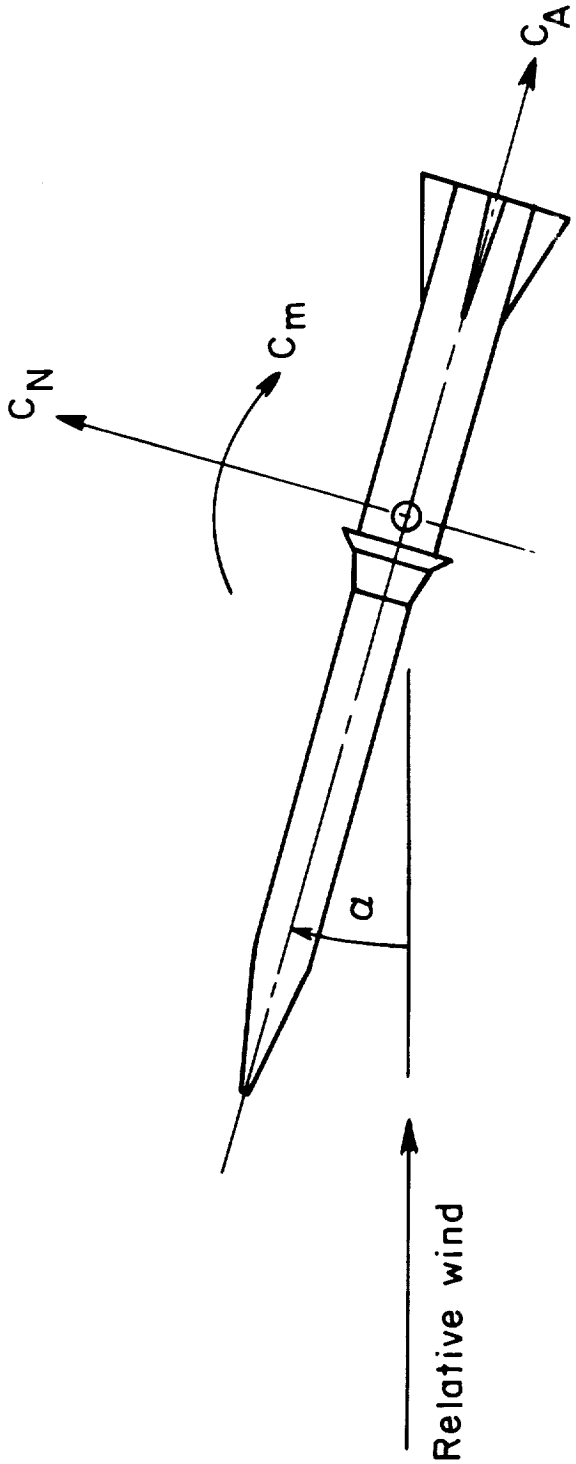

Figure 1.- Body-axis system. (Arrows indicate positive directions.)

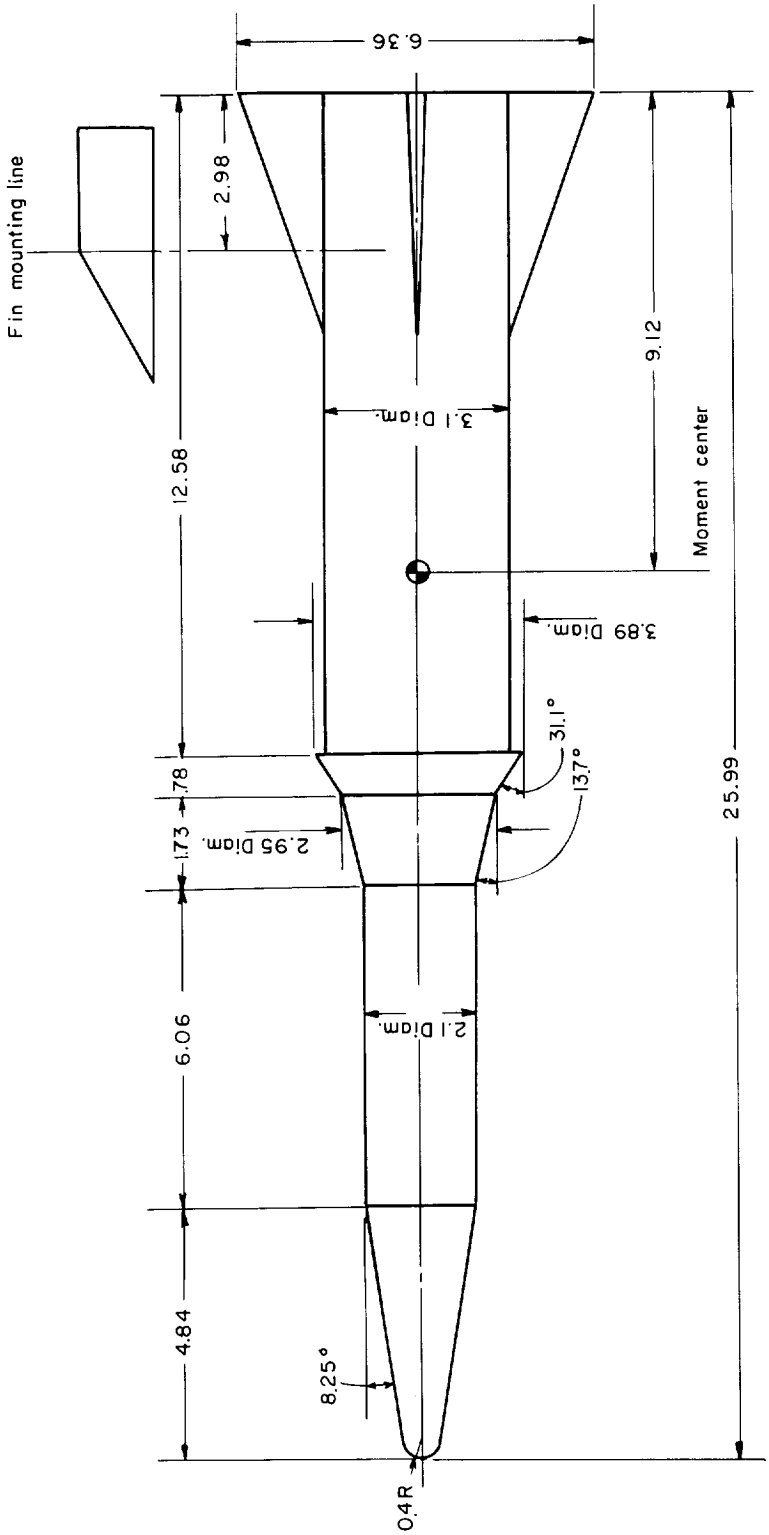

(a) Overall model.

Figure 2.- Dimensional details of a 0.10-scale rocket vehicle. (Dimensions are in inches.)

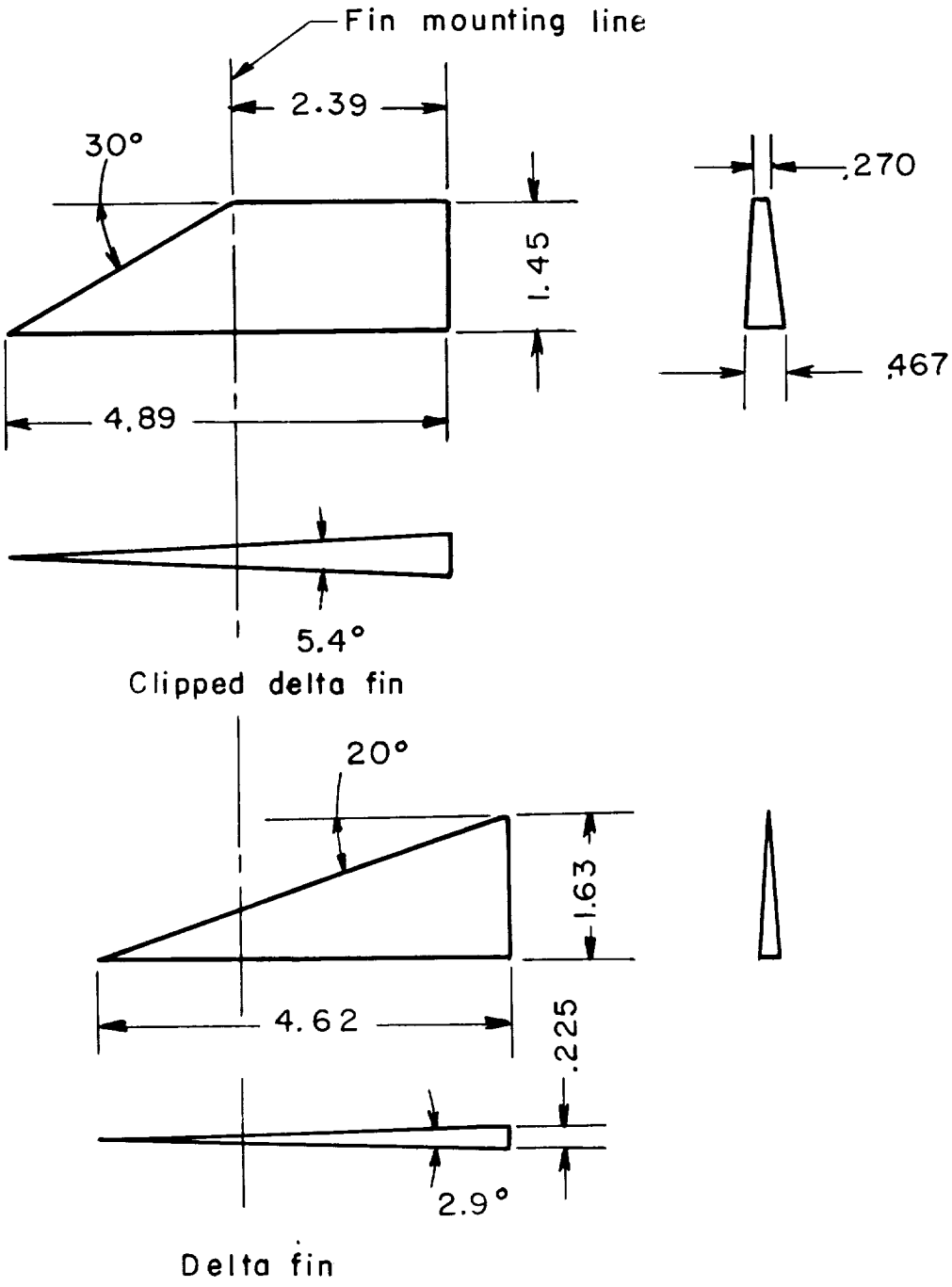

(b) Fin detail.

Figure 2.- Concluded.

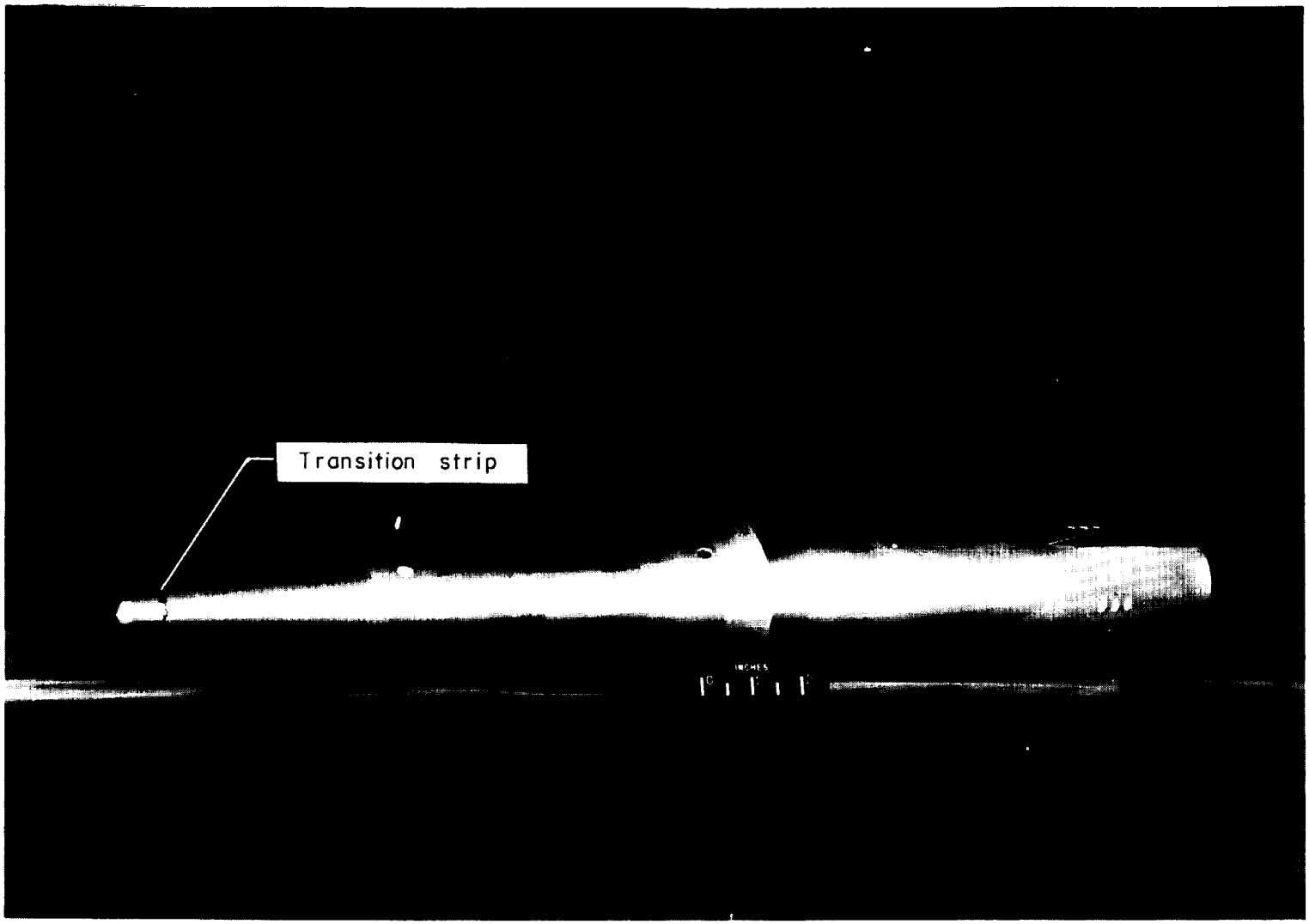

Figure 3.- Photograph of the 0.10-scale model of a rocket vehicle. L-61-3534.1

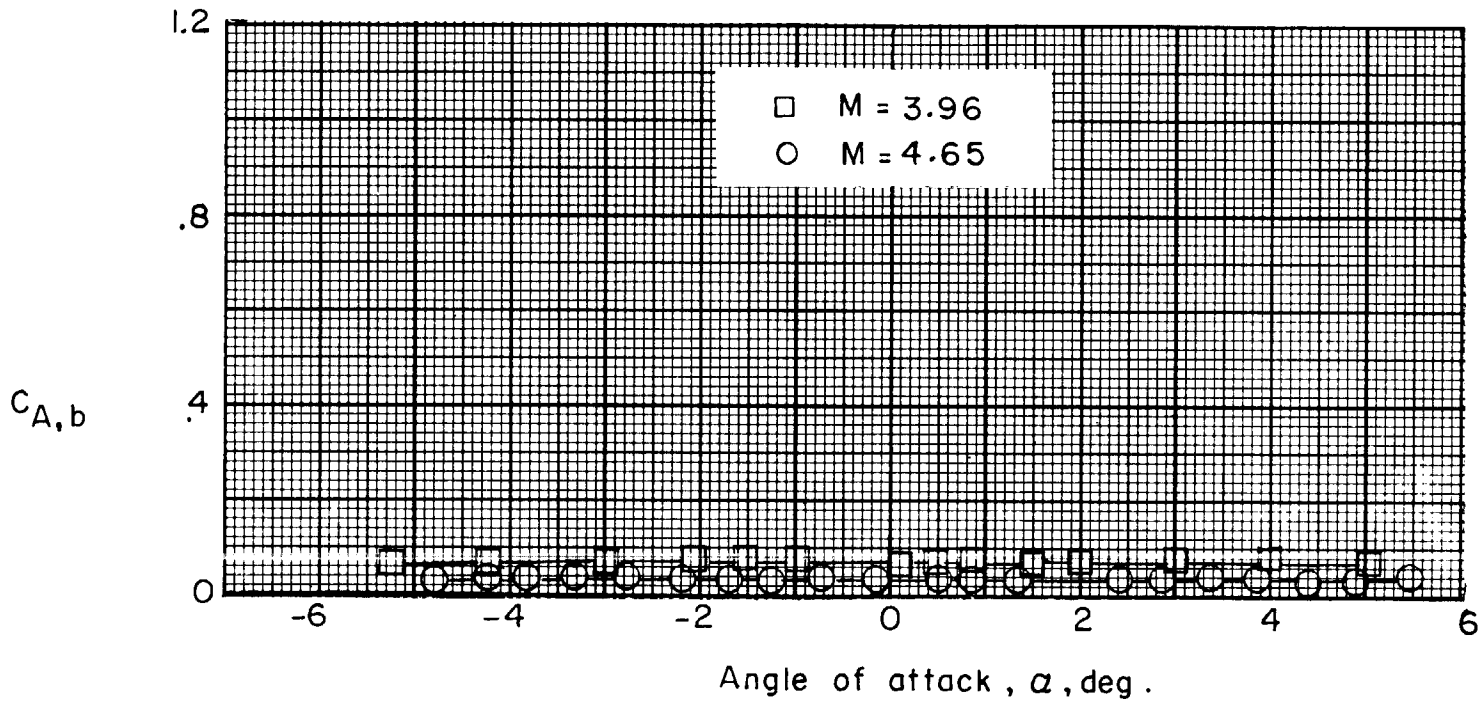

Figure 4.- Typical base axial-force coefficients for a 0.10-scale rocket vehicle.

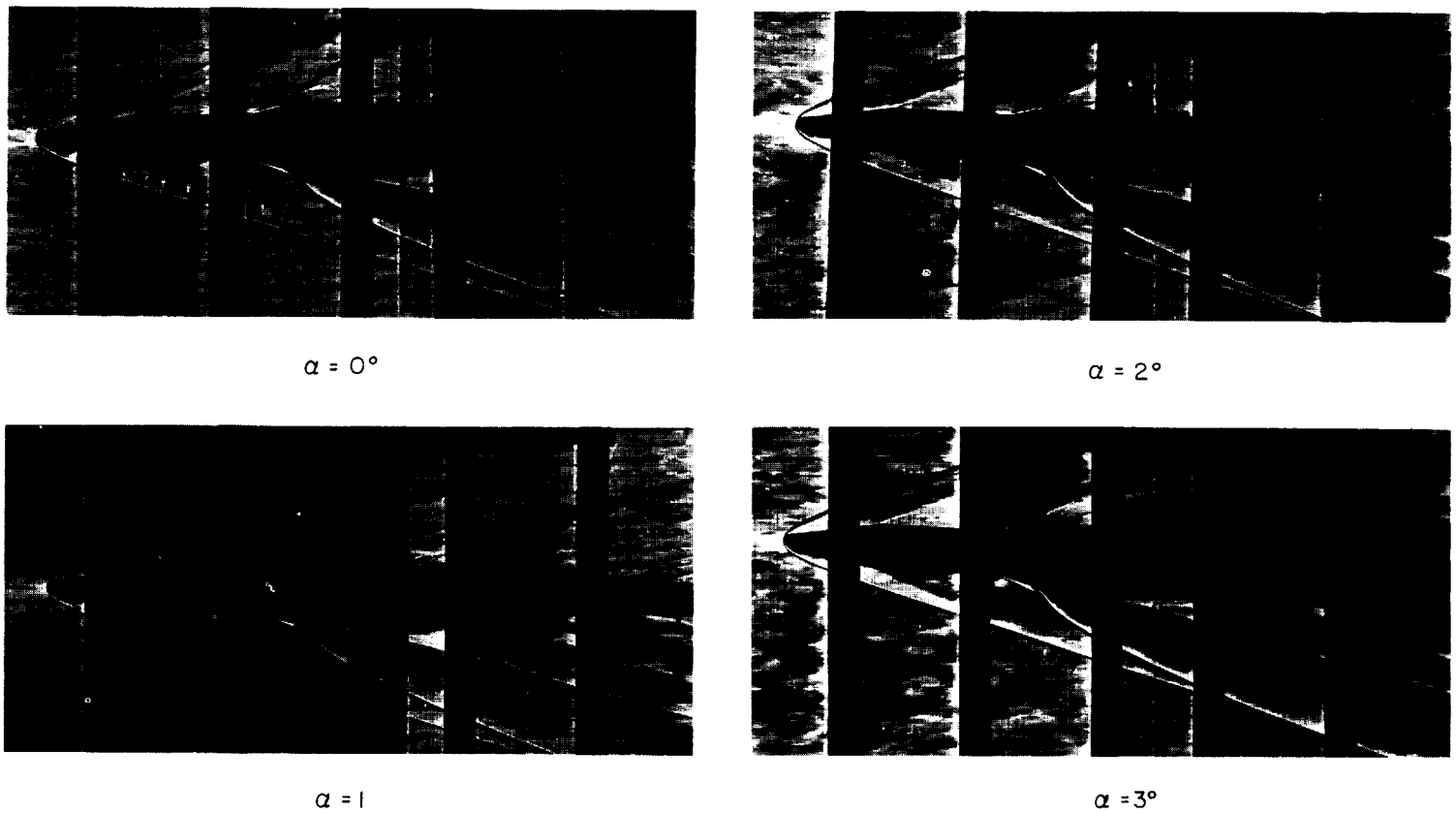

(a) Mach number 3.96. L-61-5108

Figure 5.- Schlieren photographs of the 0.10-scale model with clipped delta fins.

$\alpha = 0°$

$\alpha = 2°$

$\alpha = 1°$

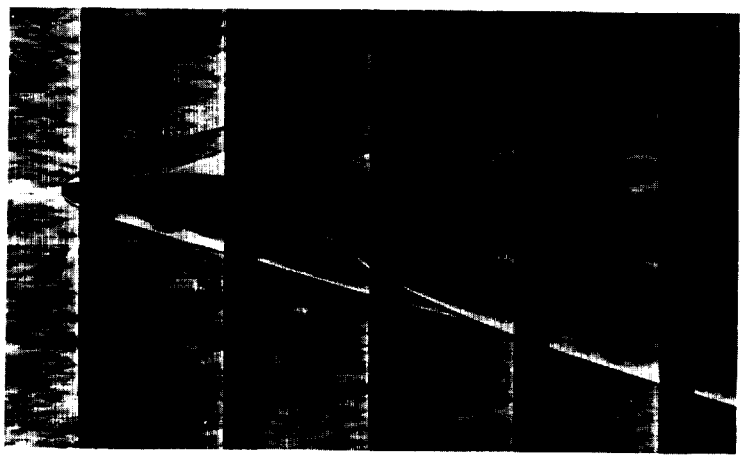

$\alpha = 3°$

(b) Mach number 4.65. L-61-5109

Figure 5.- Concluded.

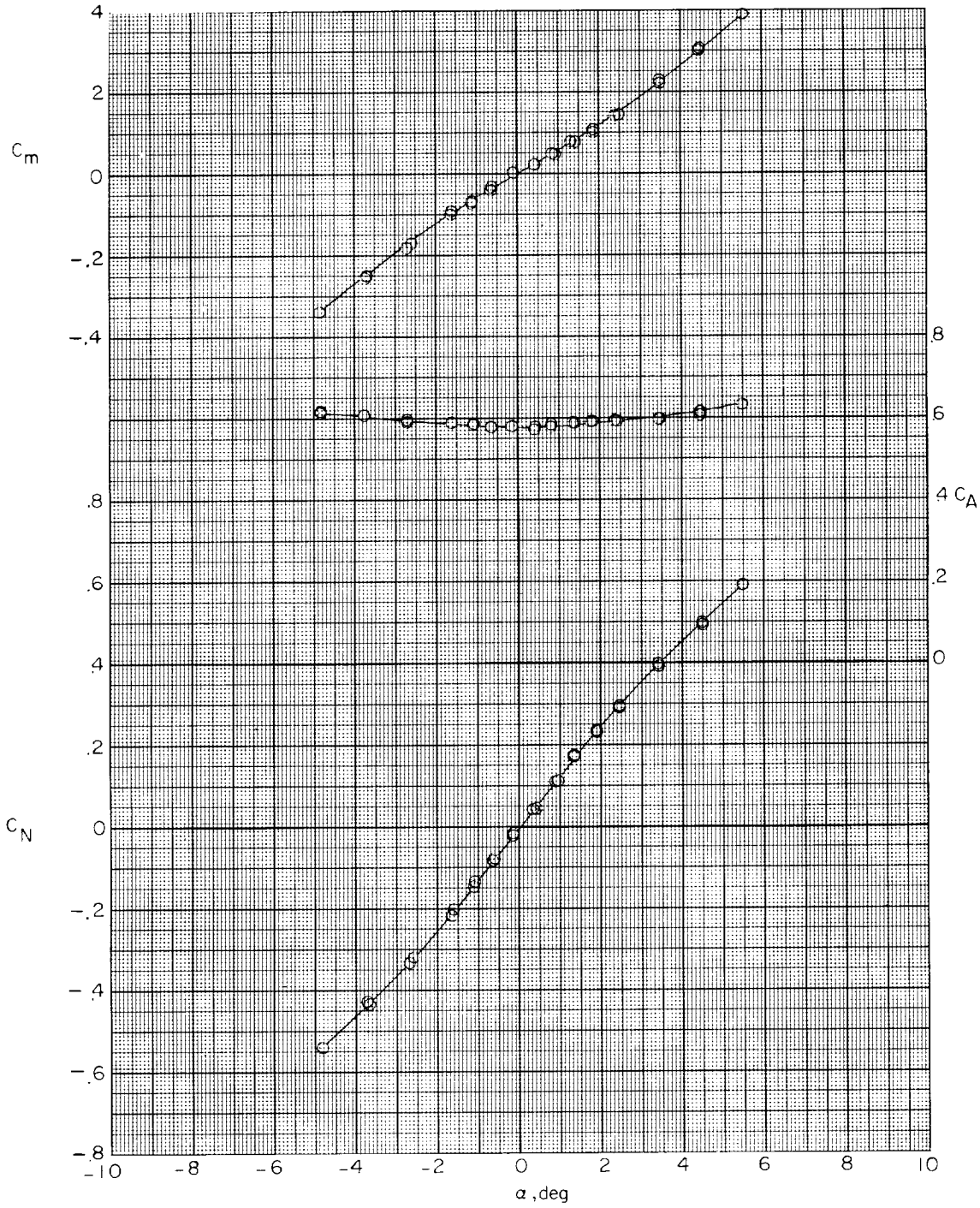

Figure 6.- Aerodynamic characteristics in pitch of the 0.10-scale model with delta fins at M = 4.65.

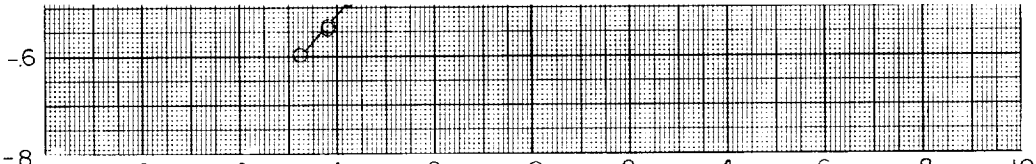

18

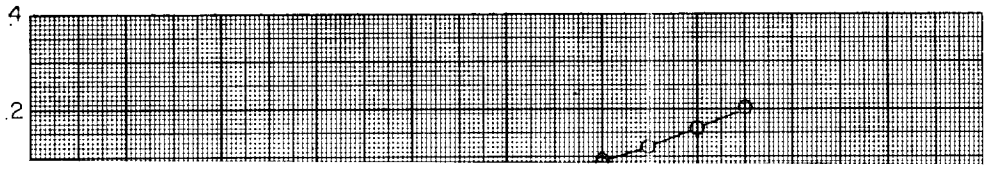
4
2

20

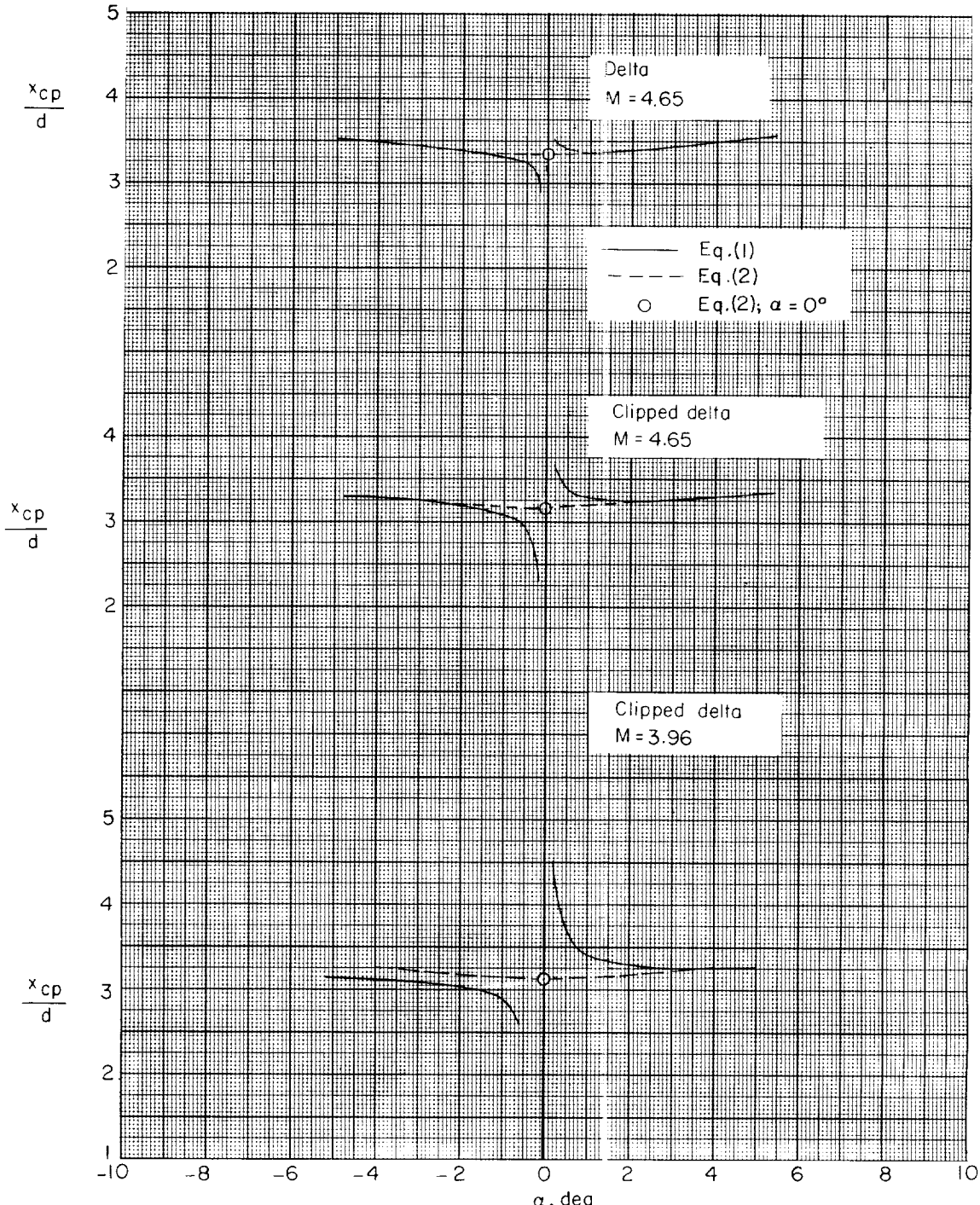
Delta
M = 4.65
Eq.(1)
Eq.(2)
Eq.(2); α = 0°
Clipped delta
M = 4.65
Clipped delta
M = 3.96
xcp/d
5
4
3
2
1
-10
-8
-6
-4
-2
0
2
4
6
8
10
α, deg

L-1036

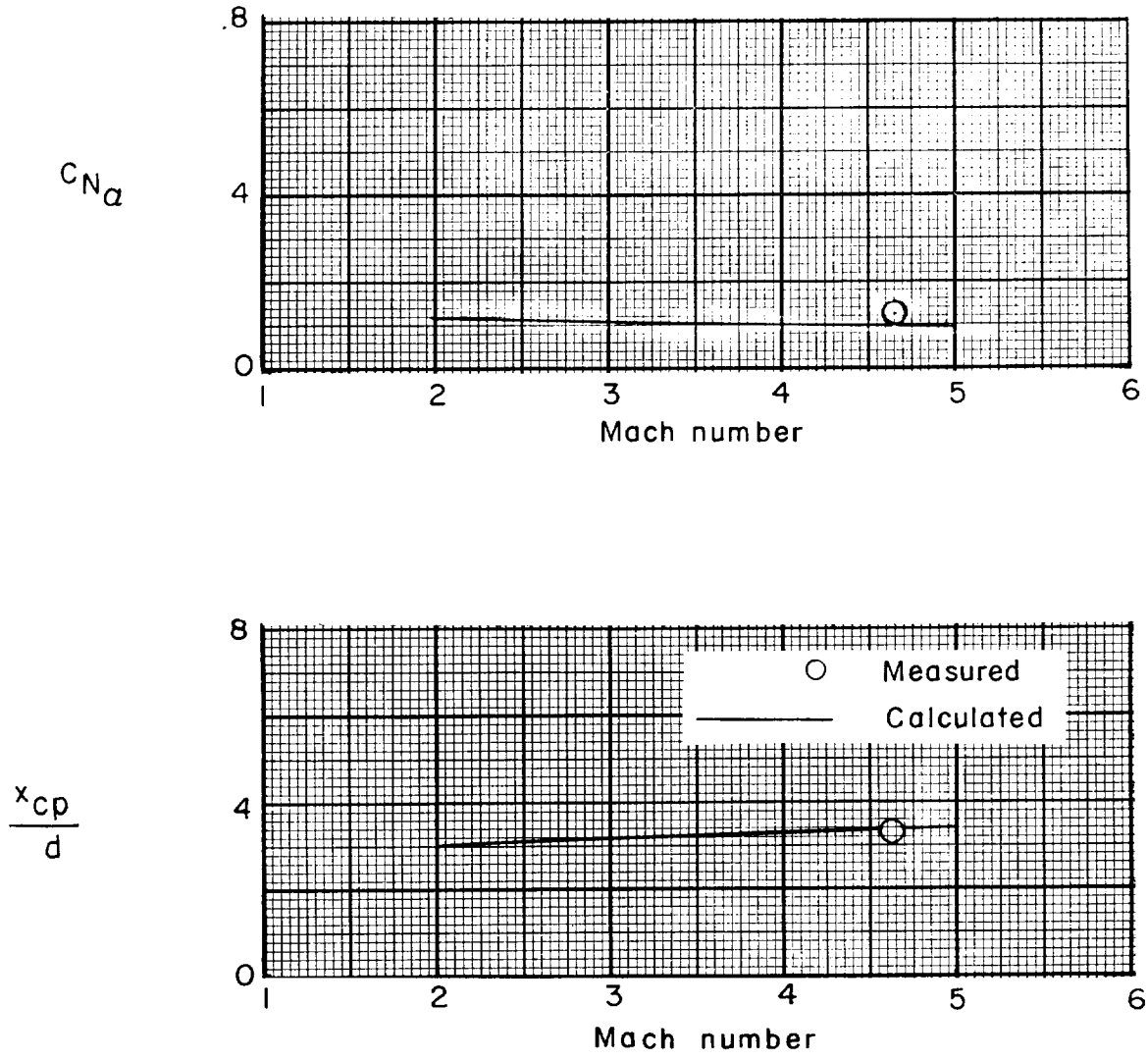

(a) Delta fins.

Figure 10.- Comparison of test results and calculated values of the static longitudinal characteristics for the 0.10-scale model of a rocket vehicle.

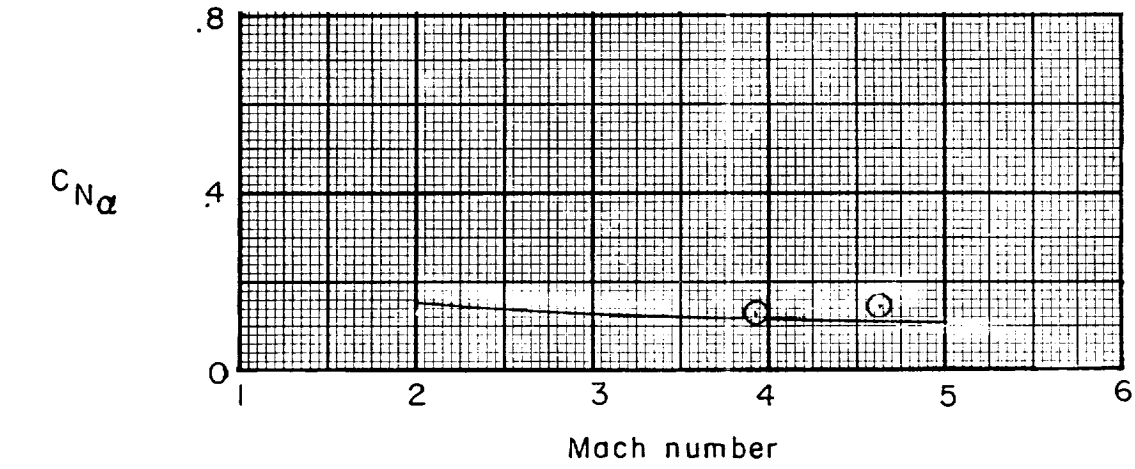

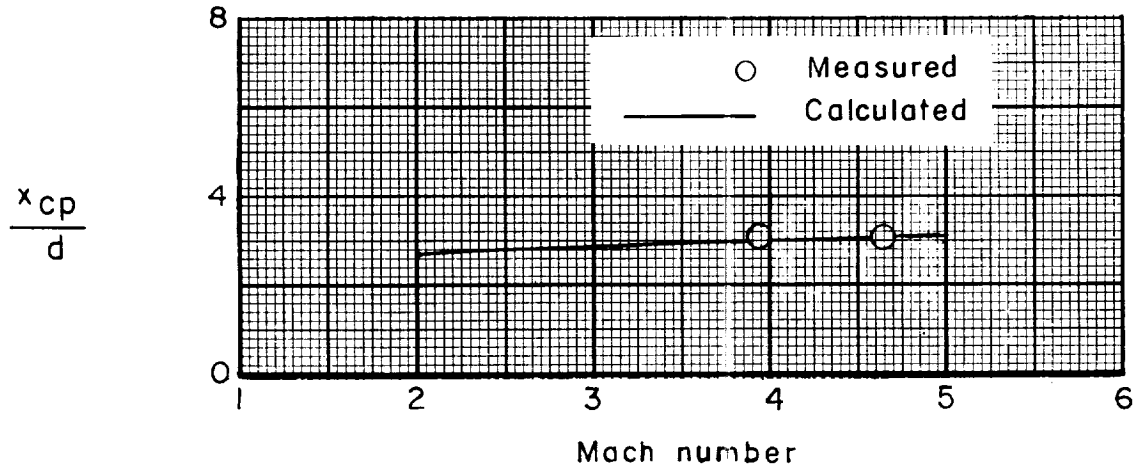

(b) Clipped delta fins.

Figure 10.- Concluded.